Geophysical Research Letters

16 JULY 2005
Volume 32 Number 13
American Geophysical Union

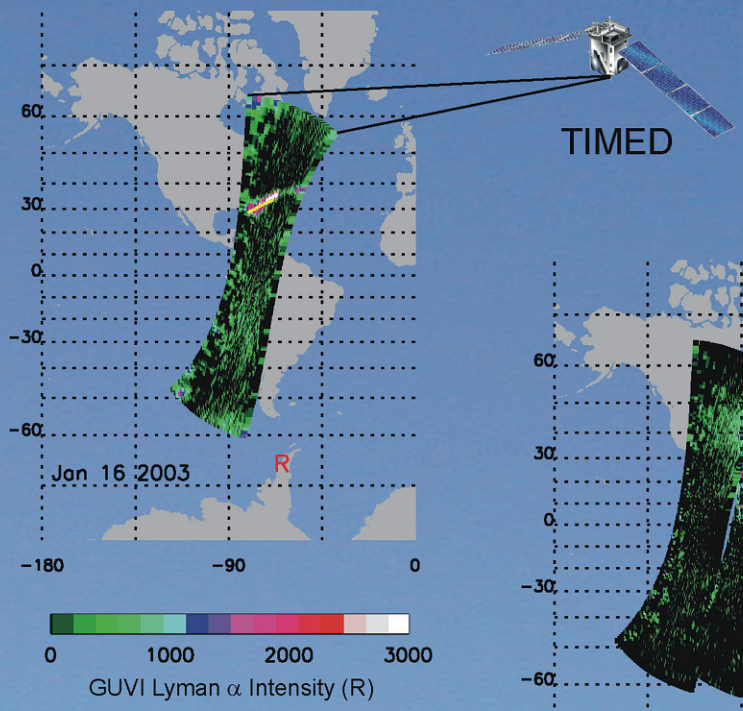

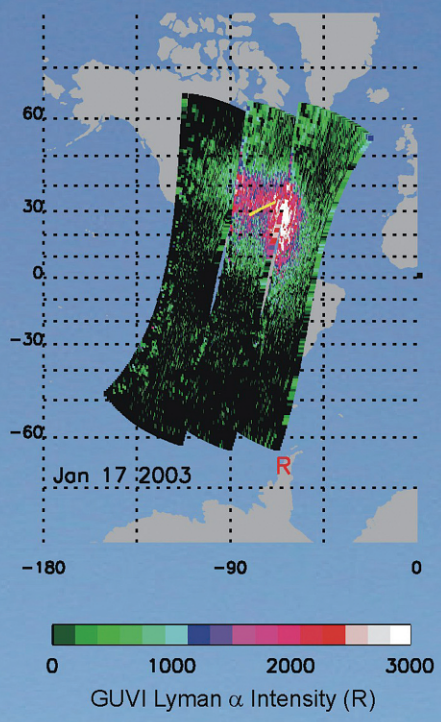

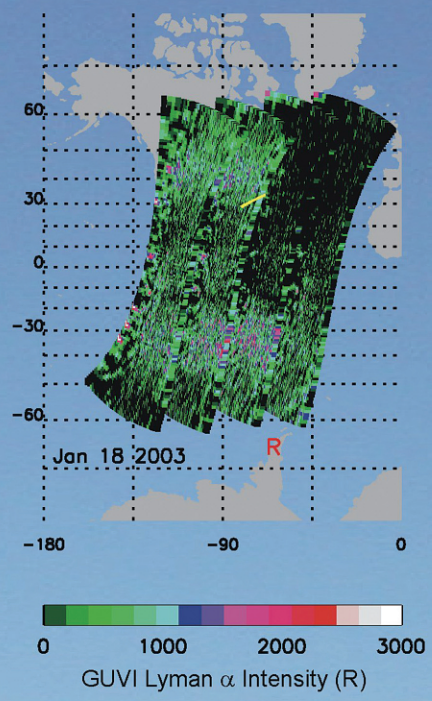

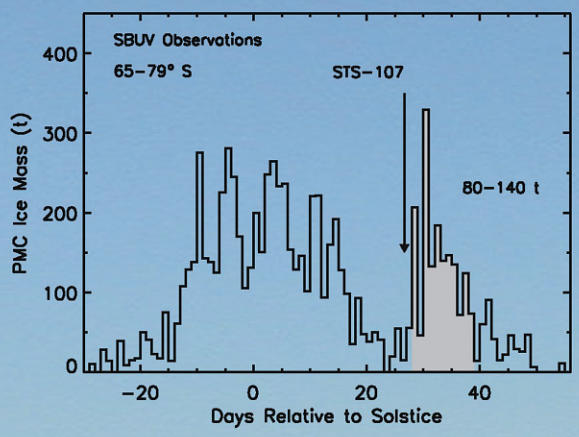

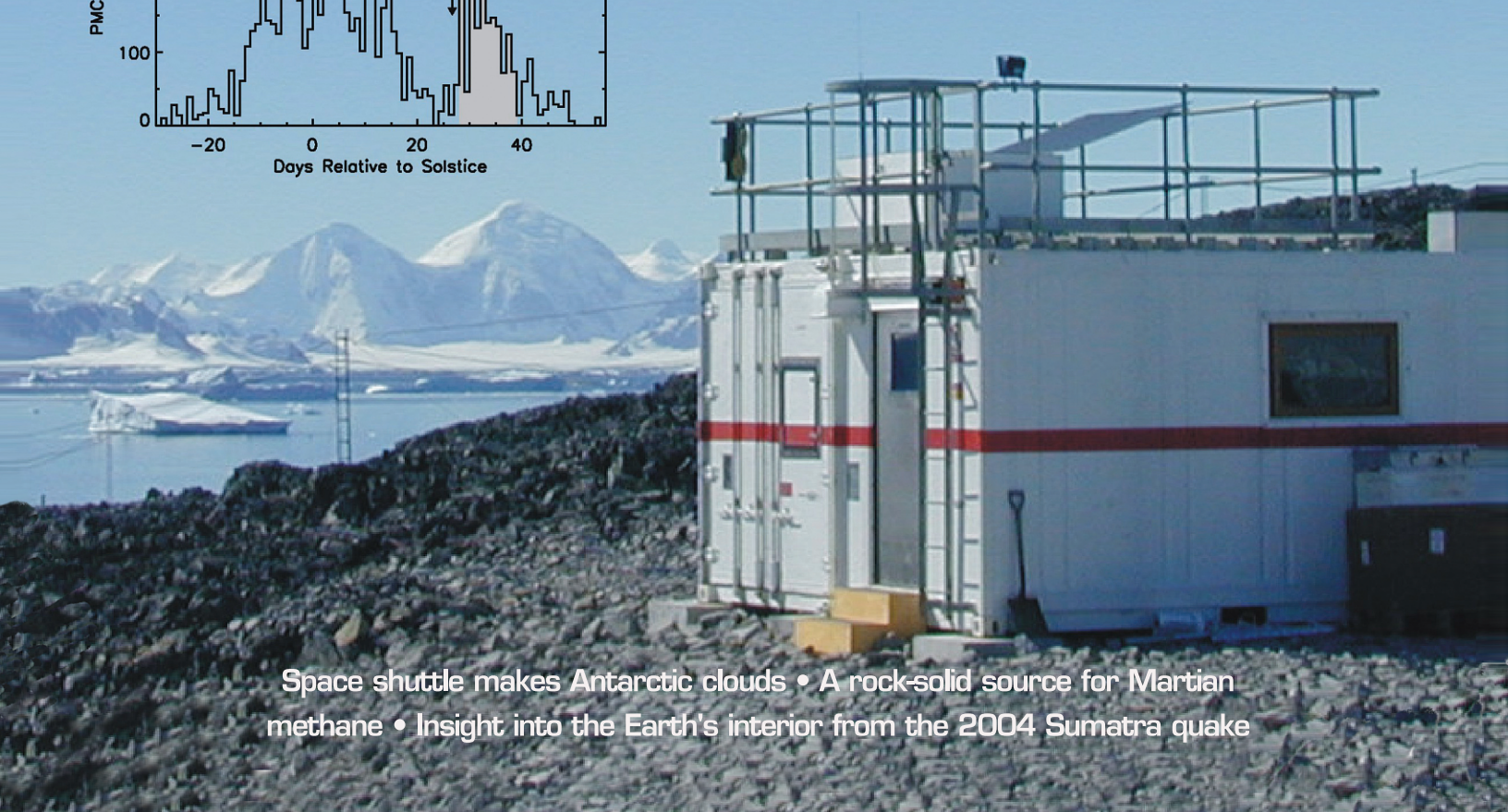

Space shuttle makes Antarctic clouds • A rock-solid source for Martian methane • Insight into the Earth's interior from the 2004 Sumatra quake

Antarctic mesospheric clouds formed from space shuttle exhaust

Michael H. Stevens
E.O. Hulburt Center for Space Research, Naval Research Laboratory, Washington, D. C., USA

R. R. Meier
School of Computational Sciences, George Mason University, Fairfax, Virginia, USA

Xinzhao Chu
Department of Electrical and Computer Engineering, University of Illinois at Urbana-Champaign, Urbana, Illinois, USA

Matthew T. DeLand
Science Systems and Applications, Inc. (SSAI), Lanham, Maryland, USA

John M. C. Plane
School of Environmental Sciences, University of East Anglia, Norwich, UK

Received 22 March 2005; revised 16 May 2005; accepted 26 May 2005; published 6 July 2005.

[1] New satellite observations reveal lower thermospheric transport of a space shuttle exhaust plume into the southern hemisphere two days after a January, 2003 launch. A day later, ground-based lidar observations in Antarctica identify iron ablated from the shuttle's main engines. Additional satellite observations of polar mesospheric clouds (PMCs) show a burst that constitutes 10–20% of the PMC mass between 65–79°S during the 2002–2003 season, comparable to previous results for an Arctic shuttle plume. This shows that shuttle exhaust can be an important global source of both PMC formation and variability. **Citation:** Stevens, M. H., R. R. Meier, X. Chu, M. T. DeLand, and J. M. C. Plane (2005), Antarctic mesospheric clouds formed from space shuttle exhaust, *Geophys. Res. Lett.*, *32*, L13810, doi:10.1029/2005GL023054.

1. Introduction

[2] Polar mesospheric clouds (PMCs) normally appear in the summer at high latitudes and are distinguished by their high altitude (~81–85 km) and tenuous composition. Sometimes called noctilucent clouds, they have been implicated as indicators of global climate change [e.g., *Thomas*, 1996], although this is disputed [*von Zahn*, 2003; *Thomas et al.*, 2003].

[3] Recently it was shown that space shuttle main engine exhaust injected near 110 km altitude on ascent can reach the Arctic to form PMCs [*Stevens et al.*, 2003]. Although one case study showed that a shuttle plume can contribute 22% to the PMC ice mass over a summer [*Stevens et al.*, 2005], data that clearly quantify this contribution are limited and there is no evidence heretofore that a shuttle plume can reach Antarctica. Any significant global-scale impact to PMCs has therefore been unsupported by observations until now.

[4] On 16 January 2003, the Columbia space shuttle (STS-107) was launched from Kennedy Space Center. The orbiter flew nearly horizontally around 110 km altitude off the east coast of the United States for about four minutes, injecting water vapor (H_2O) exhaust and trace quantities of iron (Fe) ablated from the main engines. We herein assemble observations from three different experiments to determine the fate of this lower thermospheric plume. Included are satellite observations by the Global Ultraviolet Imager (GUVI) of scattered solar Lyman α radiation near 121.6 nm and ground-based lidar observations of both Fe and PMCs from Antarctica that show rapid inter-hemispheric transport of the plume and its arrival in Antarctica, respectively. Satellite observations of PMCs by the Solar Backscatter Ultraviolet (SBUV) instrument over Antarctica show a burst of PMCs persisting up to 12 days after launch. The datasets are presented in order below.

2. Satellite Observations of the Shuttle Plume

[5] GUVI was launched aboard the NASA Thermosphere, Ionosphere, Mesosphere, Energetics and Dynamics (TIMED) satellite on 7 December 2001 [*Christensen et al.*, 2003]. GUVI can produce images of dayglow radiation by looking at the Earth's disk and scanning its field-of-view transverse to the spacecraft ground track. Atomic hydrogen produced from the dissociation of H_2O exhaust can scatter Lyman α sunlight above ~85 km altitude [*Hicks et al.*, 1999], so large-scale (>1000 km) plume motion can be inferred from the images in daily increments.

[6] Figure 1a shows a bright streak of Lyman α emission observed on 16 January, 2003 only 1.8 hours after launch. The emission peaks near 3.0 kiloRayleighs (kR) and is located by subtracting a background that is ~25 kR. Figure 1a demonstrates GUVI's ability to detect a freshly injected shuttle exhaust plume using Lyman α observations.

[7] Figure 1b shows three orbits of GUVI data obtained between 1.0–1.2 days after launch. The exhaust has apparently sheared and diffused; some of it is moving northwest but much of it is moving south toward the equator. The brightest (white) portion in Figure 1b is between 12–33°N yielding an average southward mean wind speed of 13 m/s.

Copyright 2005 by the American Geophysical Union.
0094-8276/05/2005GL023054$05.00

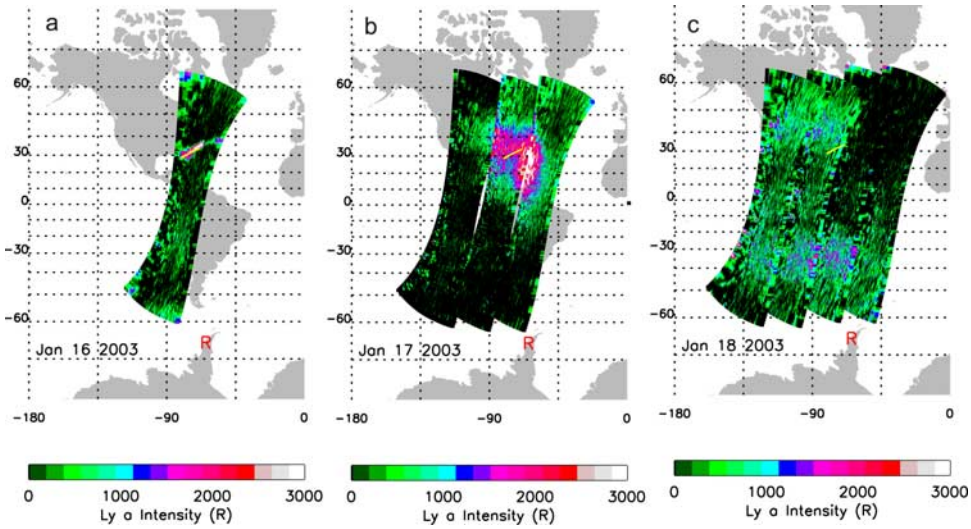

Figure 1. GUVI Lyman α observations of the STS-107 plume. The data are referenced to the color bar on the bottom where the statistical uncertainty is about ±500 R. Each pixel is 7 km square and the images have been smoothed by three pixels in each direction. The location of an Fe lidar in Rothera is indicated by an "R". (**a**) Shuttle plume 1.8 hours after launch. The white streak of emission off the U.S. east coast is adjacent to the shuttle ground track (in yellow). The main engines were cutoff near 112 km at the northeast end of the ground track. (**b**) 1.0–1.2 days after launch. A large portion of the effluents moves southward. (**c**) 1.9–2.2 days after launch. The plume is in the southern hemisphere near 35°S.

[8] Figure 1c shows four orbits of GUVI data obtained between 1.9–2.2 days after launch. These data are distinguished by a more diffuse region of emission between 27–44°S, peaking around 2.0 kR. Figures 1b and 1c imply rapid inter-hemispheric transport of the plume with a mean southward wind of 75 m/s. The average mean southward wind derived from Figures 1a–1c is therefore 44 m/s, which is about four to five times faster than those from satellite climatologies for this time of year near 110 km [*McLandress et al.*, 1996]. However, evidence of much faster winds near 110 km (>100 m/s) is typically found in more instantaneous ground-based chemical tracer observations [*Larsen*, 2002]. Clearly, mean meridional transport in the lower thermosphere is an area worthy of continued study.

3. The Shuttle Plume in Antarctica

3.1. Fe Lidar Observations

[9] Our second set of observations is from the University of Illinois Fe Boltzmann temperature lidar installed in collaboration with the British Antarctic Survey in December, 2002 at the Rothera Research Station (67.6°S and 292.0°E; "R" in Figures 1a–1c). The lidar measures time-dependent vertical profiles of Fe concentration, temperature and PMCs [*Chu et al.*, 2004]. Figure 2 shows observations from 19–20 January 2003 obtained 2.8–4.0 days after launch. The persistent ambient layer of Fe near 90 km is produced from ablating meteoroids entering the Earth's atmosphere [*Plane*, 2003]. However, there are also three higher altitude features between 104–113 km; the highest and most distinct is seen near 112 km around 00:30 UT. Fe above 110 km is very unusual at Rothera, appearing in only some 3% of the 460 hours of observations from December 2002 to August 2004 and all at lower concentrations than the peak near 112 km.

[10] This Fe is perplexing when considered in isolation. However, in the context of the GUVI observations we propose that it is within the relocated shuttle plume, and produced by the normal ablation of main engine components during launch [e.g., *van Dyke et al.*, 1992]. Not only are these high altitude features unique within the lidar dataset, but they appear at virtually the same altitudes as the injected plume and at a time that is consistent with the mean southward wind inferred from the GUVI observations in Figure 1.

3.2. The Plume Simulation

[11] For quantitative insight to the plume evolution, we employ a two-dimensional model. Between 100–115 km, where most of the observed shuttle plume is injected, molecular diffusion dominates over eddy diffusion [*Plane*,

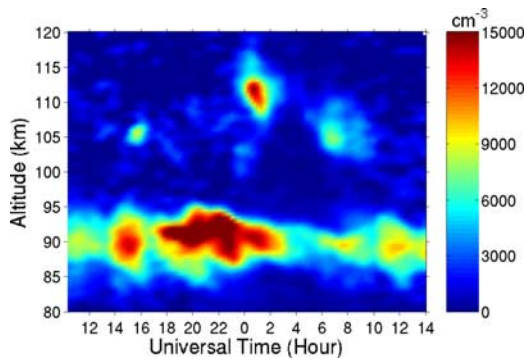

Figure 2. Fe densities over Rothera, Antarctica: 19–20 January, 2003. The observations, made 2.8–4.0 days after launch of STS-107, have a vertical resolution of ~1 km and a temporal resolution of ~1 hour. The maximum near 112 km is 1.5×10^4 cm^{-3} (±200–300 cm^{-3}). There is no known natural source of neutral Fe above 100 km.

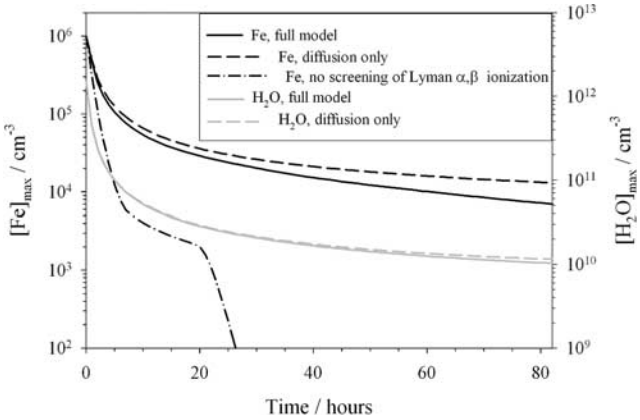

Figure 3. Peak concentrations of Fe and H_2O in shuttle plume. The predicted peak concentrations of Fe are shown as black lines (left-hand axis) and of H_2O are shown as grey lines (right-hand axis) upon arrival over Rothera. The different cases are: full model (solid lines); diffusion only, no chemistry (dashed lines); and no screening by H_2O of ionizing radiation within the plume (dash-dot-dash line). High concentrations of H_2O in the shuttle plume prolong the lifetime of both Fe and H_2O.

2004]. The model includes molecular diffusion of both H_2O and Fe, with the loss of Fe controlled by the charge transfer reactions:

$$Fe + NO^+ \rightarrow Fe^+ + NO \quad (1)$$

$$Fe + O_2^+ \rightarrow Fe^+ + O_2 \quad (2)$$

The ionization rate of Fe above 100 km is much faster than the neutralization of Fe^+ [*Plane*, 2003], so that formation of Fe^+ by reactions 1 or 2 is essentially a permanent removal of Fe. This means there is no known natural source of neutral Fe above 100 km, providing additional evidence for a shuttle source to the high altitude features in Figure 2.

[12] In the model, a circular parcel of pure H_2O is inserted at 112 km with a radius of 1.7 km. The H_2O is initialized with a concentration of 1.5×10^{12} cm^{-3} (i.e., at local atmospheric pressure) and the Fe is initialized with a concentration of 1×10^6 cm^{-3} (discussed further below). The model is run for the time period between launch and the Fe observations (81 hours). The solar illumination during this time is deduced from the GUVI observations in Figure 1 and the atmospheric conditions are varied along the projected path [*Hedin*, 1991; *Bilitza et al.*, 1993].

[13] Fe is preserved against charge transfer because the concentrations of NO^+ and O_2^+ inside the plume are substantially reduced by the high concentrations of H_2O, which extinguish ionizing Lyman α and β (102.6 nm) radiation. The black lines in Figure 3 illustrate the peak concentrations of Fe as a function of time for three different cases: the full model as described above (solid line), no charge transfer with NO^+ and O_2^+ so that Fe is dispersed by diffusion only (dashed line), and no screening of Lyman α and β radiation inside the plume (dot-dashed line). For this last case, the Fe would have fallen below the lidar detection limit in only 25 hours. Comparing the first two cases shows that the peak Fe concentration after 81 hours is reduced through charge transfer reactions by only 46%, so that an observable plume of Fe with a peak concentration of about 7×10^3 cm^{-3} should remain after 81 hours.

[14] This prediction is generally consistent with the three high altitude peaks of 5×10^3–1.5×10^4 cm^{-3} spaced 15 hours apart (Figure 2). Our initial Fe density of 1×10^6 cm^{-3} injected uniformly into a plume with a radius of 1.7 km and a length of 1000 km means that ~0.8 kg of Fe would need to have ablated from the three main engines during the four minutes spent near 110 km. This is plausible given that we are likely observing a small fraction of the plume at Rothera, preventing a reliable spatial average.

[15] The modeled peak H_2O concentrations in the plume are also shown in Figure 3 (grey lines). As with Fe, the high concentrations of H_2O in the plume protect it from solar Lyman α radiation [*Stevens et al.*, 2003] thereby prolonging its lifetime to photolysis loss so that in this case 73% of the plume remains after 81 hours. However, because the molecular diffusion coefficient of H_2O in air is a factor of two greater than that of Fe [*Self and Plane*, 2003; *Lide*, 2005], H_2O diffuses faster than Fe. The ratio of the vertical distances diffused goes as the square root of the ratio of the diffusion coefficients. Upon reaching Rothera we calculate the distance below the peak over which the effluent reaches half its peak value to be about 4.5 km for Fe, generally consistent with our observations in Figure 2, and 6–7 km for H_2O.

[16] The high concentrations of the diffused H_2O plume raise the frost point temperature [*Mauersberger and Krankowsky*, 2003] by ~10 K to 148 K at 92 km. This temperature is consistent with that over Rothera at this altitude (143–160 K) measured simultaneously [*Chu et al.*, 2004] and indicates that ice formation is possible. Indeed PMCs were observed during transit of the plume by the same lidar. Figure 4a shows the daily operational

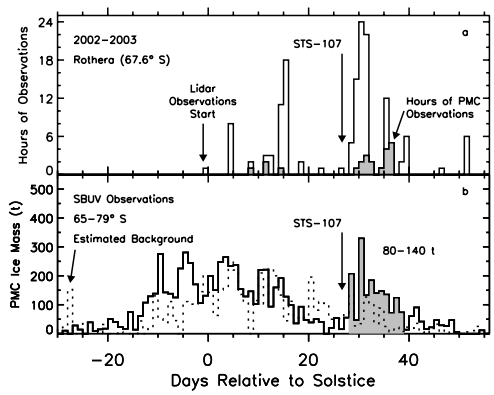

Figure 4. Antarctic PMC observations: 2002–2003. (**a**) Hours of Rothera lidar observations. The daily hours of observation varied due to inclement weather and the start time of observations is indicated. 82% of all PMCs (shaded) appeared between 3–10 days after the STS-107 launch. (**b**) SBUV PMC ice mass. The data (black histogram) is an average of NOAA-16 (ascending node) and NOAA-17 (descending node) observations. A possible background (dotted line) is estimated (see text). A burst following launch of STS-107 is shaded and the average during this time period is indicated rounded to the nearest 10 t.

hours for the 2002–2003 PMC season against days relative to solstice (DRS) as well as the daily hours of PMC observations (shaded). The altitudes of these PMCs were typical and all between 81.7–86.0 km. Their peak volume backscatter coefficient was also typical of all PMCs observed at this location between 2002–2004. A remarkable 82% of all PMCs were observed between 3–10 days after launch of STS-107, suggesting that this shuttle plume strongly influenced the appearance of PMCs at Rothera during the 2002–2003 summer. The timing of this burst can be directly compared with PMC satellite data, discussed next.

4. Satellite PMC Observations

[17] Our next dataset consists of satellite observations of PMCs by the Solar Backscatter Ultraviolet (SBUV) instrument [*DeLand et al.*, 2005]. SBUV was carrying out routine observations of PMCs over latitudes up to 82° in 2002–2003. To establish context for the shuttle plume, we first calculate the 2002–2003 seasonal variation of the PMC ice mass over the Antarctic by averaging the data from two SBUV satellites (NOAA-16 and NOAA-17). To convert the daily averaged cloud albedo to ice column abundance, we assume a log-normal distribution of spherical water ice particles with a median radius of 55 nm and a distribution width of 1.42 [*von Cossart et al.*, 1999]. The zonally integrated mass is found by multiplying by the area of interest and the daily averaged PMC frequency [*Stevens et al.*, 2005].

[18] Figure 4b shows the SBUV PMC ice mass between 65–79°S and indicates both large and small scale structure during the season. A burst of activity is nonetheless evident, persisting from 2–12 days after the shuttle launch and consistent in time with the burst in Figure 4a. We take the average PMC mass of the shaded area in Figure 4b (140 t) as an upper limit and consider the possibility that a background of ice particles is underneath. Averaging SBUV data from the year before (NOAA-16) and the year after (NOAA-17) yielded an average of 60 t of ice in the same time period. The PMC ice mass due to the shuttle exhaust is therefore found to be 80–140 t. Varying the prescribed ice particle median radius from 55 nm to between 30 and 130 nm introduces an uncertainty of only 17% to the calculated PMC ice mass [*Stevens et al.*, 2005].

[19] The ice mass in the PMC burst is consistent with what is available from the plume: STS-107 injected ~350 t of H_2O between 100–115 km, which is depleted to ~250 t on transit to Antarctica from our model results in Section 3b. Integrating all the PMC ice mass in Figure 4b, we find that the shuttle contribution is 10–20% of the total for the 2002–2003 austral summer.

5. Summary

[20] Our data show that at least 20% of the STS-107 shuttle plume injected between 100–115 km was advected to Antarctica and formed ice near the cold summer polar mesopause. Therefore, a space shuttle exhaust plume can form PMCs in Antarctica and can contribute substantially (10–22%) to the PMC mass in either polar region [*Stevens et al.*, 2005]. We have also shown that ground-based observations of Fe above 100 km can be used as a marker of a shuttle plume.

[21] It is noteworthy that during northern and southern summers there were two to three times as many successful shuttle launches in the 1990's (13–14) than in the 1980's (4–5). A positive bias to the PMC mass in the 1990's compared to the 1980's due to space shuttle exhaust can therefore not be ruled out in either hemisphere. We conclude that the evidence for an important contribution to PMCs by shuttle traffic calls into question any interpretation of late 20th century PMC trends solely in terms of global climate change.

[22] **Acknowledgments.** Support for this work was provided by the Office of Naval Research, the NASA Office of Space Science, the British Antarctic Survey and the University of Illinois. The Fe Boltzmann temperature lidar was supported by NSF grants ATM-03-034357. We thank C. S. Gardner, P. Espy, G. Nott, J. Diettrich and D.J. Maxfield for their assistance in deploying the lidar, D. van Dyke for productive discussions on plume spectroscopy, C. R. Englert for his assistance in SBUV data analysis and Mission Operations at NASA-Johnson Space Center for providing the Columbia ascent information.

References

Bilitza, D., K. Rawer, L. Bossy, and T. Gulyaeva (1993), International reference ionosphere—Past, present, and future: I. Electron density, *Adv. Space Res.*, *13*(3), 3–13.

Christensen, A. B., et al. (2003), Initial observations with the Global Ultraviolet Imager (GUVI) in the NASA TIMED satellite mission, *J. Geophys. Res.*, *108*(A12), 1451, doi:10.1029/2003JA009918.

Chu, X., et al. (2004), Lidar observations of polar mesospheric clouds at Rothera, Antarctica (67.5°S, 68.0°W), *Geophys. Res. Lett.*, *31*, L02114, doi:10.1029/2003GL018638.

DeLand, M. T., E. P. Shettle, G. E. Thomas, and J. J. Olivero (2005), A quarter century of satellite PMC observations, *J. Atmos. Sol. Terr. Phys.*, in press.

Hedin, A. (1991), Extension of the MSIS thermosphere model into the middle and lower atmosphere, *J. Geophys. Res.*, *96*, 1159–1172.

Hicks, G. T., T. A. Chubb, and R. R. Meier (1999), Observations of hydrogen Lyman α emission from missile trails, *J. Geophys. Res.*, *104*(A5), 10,101–10,109.

Larsen, M. F. (2002), Winds and shears in the mesosphere and lower thermosphere: Results from four decades of chemical release wind measurements, *J. Geophys. Res.*, *107*(A8), 1215, doi:10.1029/2001JA000218.

Lide, D. R. (Ed.) (2005), *CRC Handbook of Chemistry and Physics, Internet Version 2005*, CRC Press, Boca Raton, Fla.

Mauersberger, K., and D. Krankowsky (2003), Vapor pressure above ice at temperatures below 170 K, *Geophys. Res. Lett.*, *30*(3), 1121, doi:10.1029/2002GL016183.

McLandress, C., et al. (1996), Combined mesosphere/thermosphere winds using WINDII and HRDI data from the Upper Atmosphere Research Satellite, *J. Geophys. Res.*, *101*(D6), 10,441–10,453.

Plane, J. M. C. (2003), Atmospheric chemistry of meteoric metals, *Chem. Rev.*, *103*, 4963–4984.

Plane, J. M. C. (2004), A time-resolved model of the mesospheric Na layer: Constraints on the meteor input function, *Atmos. Chem. Phys.*, *4*, 627–638.

Self, D. E., and J. M. C. Plane (2003), A kinetic study of the reactions of iron oxides and hydroxides relevant to the chemistry of iron in the upper mesosphere, *Phys. Chem. Chem. Phys.*, *5*, 1407–1418.

Stevens, M. H., et al. (2003), Polar mesospheric clouds formed from space shuttle exhaust, *Geophys. Res. Lett.*, *30*(10), 1546, doi:10.1029/2003GL017249.

Stevens, M. H., C. R. Englert, M. T. DeLand, and M. Hervig (2005), The polar mesospheric cloud mass in the Arctic summer, *J. Geophys. Res.*, *110*, A02306, doi:10.1029/2004JA010566.

Thomas, G. E. (1996), Is the polar mesosphere the miner's canary of global change?, *Adv. Space Res.*, *18*(3), 149–158.

Thomas, G. E., J. J. Olivero, M. T. DeLand, and E. P. Shettle (2003), Comment on "Are noctilucent clouds truly a 'miner's canary' for global change?", *Eos Trans. AGU*, *84*, 352.

van Dyke, D. B., G. D. Tejwani, F. E. Bircher, and T. J. Cobb (1992), SSME plume spectral data obtained during ground testing at SSC: Analysis and correlation with engine operating characteristics, *NASA Conf. Publ.*, *CP-3174*, 313–326.

von Cossart, G., J. Fiedler, and U. von Zahn (1999), Size distributions of NLC particles as determined from 3-color observations of NLC by ground-based lidar, *Geophys. Res. Lett.*, *26*(11), 1513–1516.

von Zahn, U. (2003), Are noctilucent clouds truly a 'miner's canary' for global change?, *Eos Trans. AGU*, *84*, 261.

X. Chu, Department of Electrical and Computer Engineering, University of Illinois at Urbana-Champaign, Urbana, IL 61801, USA.

M. T. DeLand, Science Systems and Applications, Inc. (SSAI), Lanham, MD 20706, USA.

R. R. Meier, School of Computational Sciences, George Mason University, Fairfax, VA 22030, USA.

J. M. C. Plane, School of Environmental Sciences, University of East Anglia, Norwich NR4 7TJ, UK.

M. H. Stevens, E.O. Hulburt Center for Space Research, Naval Research Laboratory, Washington, DC 20375, USA. (stevens@uap2.nrl.navy.mil)